Shear elasticity of $K_xRb_{1-x}CN$ mixed crystals

C. W. Garland, J. O. Fossum, and A. Wells

*Department of Chemistry and Center for Material Science and Engineering, Massachusetts Institute of Technology,
Cambridge, Massachusetts 02139*

The c_{44} shear elastic constant has been measured at 10 MHz in the cubic high-temperature phase of $K_xRb_{1-x}CN$ single crystals. As the consequence of a bilinear coupling term in the free energy, c_{44} is the soft mode associated with orientational ordering of the CN^- ions at low temperatures. The behavior of c_{44} as a function of composition and temperature has been analyzed in terms of an elastic Curie-Weiss expression and an extended mean-field model that includes quenched random strain fields. The critical temperature $T_c(x)$ for long-range ordering exhibits a roughly parabolic dependence on x, which can be modeled empirically with regular solution theory.

I. INTRODUCTION

At room temperature pure potassium cyanide, pure rubidium cyanide, and mixed crystals of $K_xRb_{1-x}CN$ $(0 < x < 1)$ possess time-averaged pseudocubic rocksalt structures $(Fm3m)$ where the dumbbell-shaped CN^- ions jump rapidly between orientational local potential minima.[1] A physically crucial factor in these crystals and in other mixed cyanide systems $(KCN_xBr_{1-x}$, $RbCN_xBr_{1-x}$, $K_xNa_{1-x}CN$, etc.) is the strong coupling between cyanide rotational degrees of freedom and lattice strains, both of quadrupolar symmetry.[1,2] This so-called translational-rotational (TR) coupling gives rise to a lattice-mediated CN^--CN^- coupling which, upon cooling, triggers a weakly first-order phase transition in the pure materials KCN and RbCN and in $K_xRb_{1-x}CN$.[3] At these elastic transitions, the cyanide ions order orientationally to yield a parallel array but no electric dipolar (i.e., head-to-tail) ordering occurs.[4] Due to the bilinear TR quadrupole coupling, the c_{44} shear elastic constant for the disordered phase softens dramatically upon cooling toward the orientational transition temperature.

In the case of diluted cyanide mixtures such as KCN_xBr_{1-x}, long-range orientational order is only observed for x values greater than a critical cyanide concentration x_c. For $x < x_c$, a quadrupolar orientational glass is observed at low temperatures.[1,5] In the latter case, quenched random strains due to the presence of substitutional ions prevent orientational long-range order well before the percolation limit x_p is reached. In a recent theory for mixed cyanide crystals, Michel[6,7] has proposed a modified static susceptibility in which the effects of random quenched strains are included in terms of a lowest-order high-temperature correction to the underlying mean-field behavior. This theoretical form has recently been verified experimentally for several diluted cyanide mixtures.[8]

It is consequently of considerable interest to investigate the effect of random strains in $K_xRb_{1-x}CN$ mixtures. Potassium and rubidium have quite similar atomic radii, $r_K/r_{Rb}=0.9$. In this case the quenched strain is too weak to destroy the macroscopic elastic ordering for any value of x, as indicated by the phase diagram shown in Fig. 1. In contrast to this, a quadrupolar glass phase has been reported[2] for $K_xNa_{1-x}CN$ mixed crystals in the range $0.15 < x < 0.9$. This is not surprising since $r_K/r_{Na}=1.4$ and the random strains must be large.

TA[100] acoustic velocity measurements have been reported previously for KCN (Ref. 9) and RbCN (Ref. 10) and the c_{44} variations in these samples are characterized by elastic Curie-Weiss behavior. The present work involves measurements of low-frequency (~ 10 MHz) TA[100] acoustic velocities in the cubic high-temperature phase of four mixed $K_xRb_{1-x}CN$ single crystals. The softening of this c_{44} shear mode in the mixed crystals will be analyzed in terms of an elastic Curie-Weiss equation and several variants of Michel's quenched-random-strain model. In all cases, the fits yield second-order transition
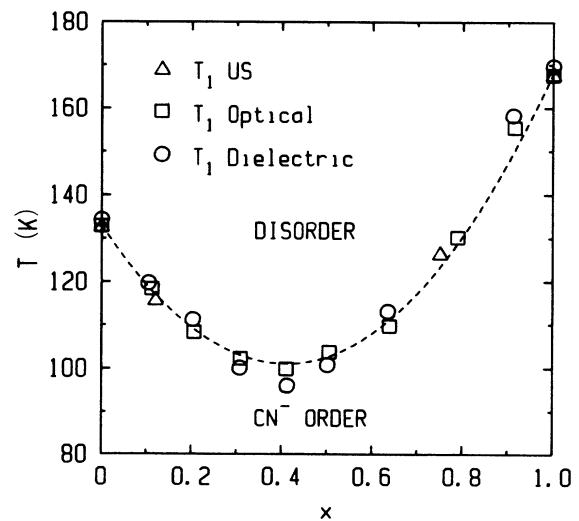

FIG. 1. Phase diagram for CN^- orientational ordering in $K_xRb_{1-x}CN$ single crystals. The transitions are all weakly first order. The transition temperatures T_1 (optical) and T_1 (dielectric) are taken from Ref. 2. The T_1 (ultrasonic) values have been obtained from the present work.

temperatures T_c which always lie below the first-order elastic transition temperature T_1. Furthermore, it is found that the composition dependence of T_c deviates from ideal solution behavior and can be described reasonably well by regular solution theory.

In Sec. II we present a review of the relevant theoretical models. The experimental procedures are discussed and the data are presented in Sec. III. The data analysis is described in Sec. IV, and some concluding remarks are given in Sec. V.

II. REVIEW OF THEORY

A. Curie-Weiss behavior

The softening of the c_{44} elastic constant for a number of alkali cyanide mixtures has been analyzed previously[11,12] with a mean-field theory based on a Landau free-energy expansion of the form

$$F = F_0 + \tfrac{1}{2}\alpha(T - T_0)Y^2 + \gamma Y\epsilon_4 + \tfrac{1}{2}c_{44}^0\epsilon_4^2 , \tag{1}$$

where F_0, α, and γ are taken to be constants (temperature independent but functions of x), T is the temperature, and Y is the cyanide orientational order parameter of quadrupolar symmetry. T_0 is the temperature at which the cyanide ions would undergo quadrupolar order in the absence of the bilinear coupling between Y and ϵ_4 shear strains, and c_{44}^0 is the bare elastic constant that one would expect in the absence of bilinear coupling. This form for F leads to the familiar Curie-Weiss expression for the c_{44} shear elastic constant:

$$\frac{c_{44}}{c_{44}^0} \equiv \frac{s_{44}^0}{s_{44}} = \frac{T - T_c}{T - T_0} , \tag{2}$$

where the elastic compliance $s_{44} \equiv 1/c_{44}$ and the bare elastic compliance $s_{44}^0 \equiv 1/c_{44}^0$. Equation (2) implies that c_{44} goes to zero at a second-order transition temperature T_c, where

$$T_c = T_0 + \frac{\gamma^2}{\alpha c_{44}^0} . \tag{3}$$

In the case of cyanide crystals, T_c represents an extrapolated hypothetical second-order transition temperature since the actual transition is first order and occurs at a temperature $T_1 > T_c$. This first-order character is due to the presence of third-order invariants (Y^3 terms) omitted from Eq. (1).[3,7] Michel and Rowe have derived Eqs. (2) and (3) starting from a microscopic model for cyanide crystals and extracting the thermodynamics from a mean-field analysis.[3]

In pure cyanides like KCN, RbCN, and NaCN, Eq. (2) appears to give a good description of the c_{44} softening induced by quadrupolar orientational interactions. This confirms the validity of mean-field theory in these systems, as expected since the upper critical dimensionality $d^* < 3$ for such elastic phase transitions.[13]

For the purpose of displaying experimental data, it is convenient to rewrite Eq. (2) in the following form:

$$\frac{1}{s_{44} - s_{44}^0} = \frac{c_{44}^0}{T_c - T_0}(T - T_c) = \frac{\alpha(c_{44}^0)^2}{\gamma^2}(T - T_c) . \tag{4}$$

It should be noted that, in general, the excess compliance $s_{44} - s_{44}^0$ is a direct measure of the collective orientational susceptibility χ.[7] Equation (4) naturally shows a linear T dependence for $1/(s_{44} - s_{44}^0)$ since a simple Landau model yields $\chi \sim (T - T_c)^{-1}$. However, the experimental variation of $s_{44} - s_{44}^0$ should indicate the actual behavior of χ in more complex systems such as the present mixed crystals.

B. Random quenched strains

Michel has extended the mean-field theory summarized above to include random static strains.[7] The random strains are assumed to play an important role in mixed cyanide crystals, where they are induced by the difference in ionic radii between substitutional ions. An independent derivation and a discussion of the basic assumptions underlying Michel's random-strain-field theory are given in a recent paper on $RbCN_xBr_{1-x}$ mixed crystals.[14] Here we will merely summarize the main theoretical results.

The lowest-order correction due to random strain fields enters through the single-particle susceptibility χ^0. This quantity is replaced by $\chi^0(1-q)$, where $q(x,T)$ is a quenched random-strain-field–induced Edwards-Anderson order parameter with the high-temperature form

$$q = \frac{\Sigma}{T^2} . \tag{5}$$

The composition dependence of Σ for diluted cyanides such as KCN_xBr_{1-x} is predicted to be $\Sigma = x(1-x)\Sigma_0$, where Σ_0 is effectively a constant (neglecting a possible very weak temperature dependence).[7] The factor $x(1-x)$ arises from the assumed random distribution of substitution ions in mixed crystals, and thus the same composition dependence should also occur in undiluted crystals like $K_xRb_{1-x}CN$. When this strain-induced parameter q is present, Eq. (2) becomes

$$\frac{c_{44}}{c_{44}^0} = \frac{s_{44}^0}{s_{44}} = \frac{T - T_c(x)(1-q)}{T - T_0(x)(1-q)} . \tag{6}$$

Mixed crystals of both the ACN_xX_{1-x} and $A_xB_{1-x}CN$ type possess the inherent possibility of quenched random strain fields due to the inequality of the radii of the substitutional ions. The "strength" Σ_0 characterizing the width of the random-field distribution has been estimated theoretically and experimentally only for the diluted-type crystals $RbCN_xBr_{1-x}$, KCN_xBr_{1-x} and KCN_xCl_{1-x}.[8,14] For a detailed discussion of Σ and Σ_0, see Ref. 7. Thus, the magnitude of the parameter Σ_0 is presently unknown for $K_xRb_{1-x}CN$ mixed crystals, although we might expect it to be fairly close to that for KCN_xCl_{1-x} since the ratio r_K/r_{Rb} is close to r_{Cl}/r_{CN}.

In the diluted cyanide crystals KCN_xBr_{1-x}, KCN_xCl_{1-x}, and $RbCN_xBr_{1-x}$, mean-field percolation gives $T_c(x) = xT_{c1}$ and $T_0(x) = xT_{01}$, where $T_{c1} = T_c(x=1)$ and $T_{01} = T_0(x=1)$ are the transition-temperature parameters of the pure cyanide. In crystals of the type $A_xB_{1-x}CN$, where there is no cyanide dilu-

tion but the two pure crystals ($x=0$ and 1) have different pseudospin interaction constants, one might expect a linear variation in T_c and T_0:

$$T_c(x)=xT_{c1}+(1-x)T_{c0} ,$$ (7a)

$$T_0(x)=xT_{01}+(1-x)T_{00} .$$ (7b)

The validity of these simple interpolation formulas will be discussed in Sec. II C and in connection with the data analysis in Sec. IV.

C. Regular solution theory

In the preceding section we discussed the quenched-random-strain-field model and the expected composition (x) dependence of the fitting parameters appearing in Eq. (6). These predictions have been verified experimentally for a number of diluted cyanide systems—$RbCN_xBr_{1-x}$, KCN_xBr_{1-x}, and KCN_xCl_{1-x}.[8] In the present case, however, the data analysis given in Sec. IV will show that Eqs. (5)–(7) do not give a good representation of the $K_xRb_{1-x}CN$ experimental data. We therefore present an alternative approach to the quadrupolar ordering process and the c_{44} shear elastic softening in undiluted cyanide crystals from the point of view of a phenomenological regular solution model.

Although both ACN_xX_{1-x} and $A_xB_{1-x}CN$ are derived from the same "parent" system ACN and have similar possibilities of nonzero Σ_0 due to random strains, there are important differences between these two kinds of mixed crystals. First, there is no cyanide dilution and thus no percolation aspect in the case of $A_xB_{1-x}CN$. Naturally, this suggests high critical ordering temperatures $T_c(x)$ over the entire composition range ($0<x<1$), as assumed in Eq. (7a). A second and highly relevant difference between $A_xB_{1-x}CN$ and ACN_xX_{1-x} arises from the fact that only a single type of CN^--CN^- nearest-neighbor coupling constant J is present in ACN_xX_{1-x} crystals, whereas three types of nearest-neighbor CN^- couplings exist in $A_xB_{1-x}CN$ mixed crystals. This is illustrated in Fig. 2, where a simplified two-dimensional representation of the $A_xB_{1-x}CN$ lattice is shown.

In the following discussion we will assume that the nearest-neighbor lattice-mediated quadrupolar CN^--CN^- coupling takes place only through the cationic sites lying adjacent to the direct "line of sight" between a given pair of cyanide ions. Thus for the two circled cyanide ions in Fig. 2, the relevant cationic sites are the ones marked 1 and 2. We further assume that the cationic sites are randomly occupied by A^+ and B^+ throughout the sample. The probability of finding an A^+ ion or a B^+ ion at any given cationic site is $P_A=x$ or $P_B=1-P_A=1-x$, where x denotes the mole fraction of positive ions that are A^+. Finally, we assume that the coupling constant J between nearest-neighbor cyanides depends on the occupation of adjacent cationic sites (sites 1 and 2 in Fig. 2). Thus there are three different CN^--CN^- coupling constants in the $A_xB_{1-x}CN$ crystal: J_{AA}, J_{BB}, and $J_{AB}=J_{BA}$, where the subscripts denote the adjacent cationic site occupation.
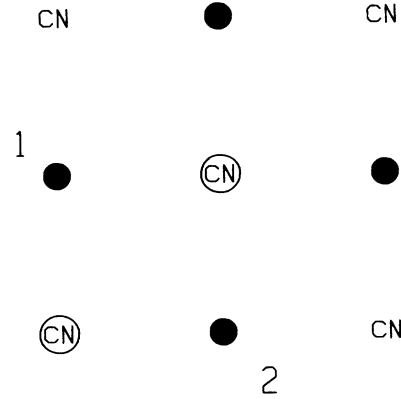

FIG. 2. Two-dimensional [(001) plane] view of an alkali cyanide lattice with the rocksalt structure, where ● represents any alkali ion. In the regular solution approximation, the effective orientational interaction between the two circled CN^- ions is assumed to depend on the nature of the alkali ions occupying the two "adjacent" cationic sites labeled 1 and 2.

The way in which a quenched random strain field can be included in a mean-field theory of quadrupolar cyanide ordering is described in Refs. 7 and 14. That analysis led to the following form for the quadrupolar orientational susceptibility:

$$\chi=\frac{1-q}{T-T_c(1-q)} ,$$ (8)

where q is the random-field-induced Edward-Anderson order parameter, $T_c=zJ/k$ is the critical ordering temperature in the absence of the random strain field, z is the CN^--CN^- coordination number, and J is the effective nearest-neighbor CN^--CN^- lattice-mediated quadrupolar coupling constant. In Refs. 8 and 14, where data on ACN_xX_{1-x} crystals were analyzed, $z=12x$ and only a single type of J (J_{AA} in the present notation) had to be considered since all the cationic sites were occupied by A^+ ions. For $A_xB_{1-x}CN$ crystals, one has

$$T_c=\frac{z}{k}(P_A^2J_{AA}+P_B^2J_{BB}+2P_AP_BJ_{AB})$$

$$=\frac{z}{k}[x^2J_{AA}+(1-x)^2J_{BB}+2x(1-x)J_{AB}] .$$ (9)

Introducing the convenient definitions $T_c^{AA}\equiv zJ_{AA}/k$, $T_c^{BB}\equiv zJ_{BB}/k$, and $T_c^{AB}\equiv zJ_{AB}/k$, one can rewrite Eq. (9) in the form

$$T_c(x)=xT_c^{AA}+(1-x)T_c^{BB}-2x(1-x)\Delta T_c^{AB} ,$$ (10)

where

$$\Delta T_c^{AB}\equiv\tfrac{1}{2}(T_c^{AA}+T_c^{BB})-T_c^{AB} .$$ (11)

The result given in Eq. (10) shows that the $T_c(x)$ behavior is parabolic rather than a simple linear interpolation between the $T_c(0)$ and $T_c(1)$ values if the parameter $\Delta T_c^{AB}\neq0$. ΔT_c^{AB} will equal zero only if the coupling constant J_{AB} is accidentally equal to the arithmetic mean of the coupling constants J_{AA} and J_{BB}. A positive (negative)

value for ΔT_c^{AB} means that the effective CN^--CN^- quadrupolar coupling is weakened (strengthened) relative to the simple interpolation average when different-sized cations are on sites 1 and 2 in Fig. 2.

The above model and the resulting Eq. (10) corresponds to an application of regular solution theory, which is commonly used to describe nonideal binary solutions. The site occupations are random (thus the entropy of mixing has the ideal value), but there are nonideal energy effects (the enthalpy of mixing, which is proportional to $\Delta J = \frac{1}{2}J_{AA} + \frac{1}{2}J_{BB} - J_{AB}$, is nonzero). Our treatment of the variation in CN^--CN^- pair interaction energy with the occupancy of "adjacent" cationic sites is different from the random interactions encountered in spin-glass systems. In our regular solution model, J represents an averaged interaction coefficient that is isotropic and does not vary with the spatial site location. The relation given in Eq. (3) shows that T_c is the net effect of two contributions: the *bare* transition temperature T_0 plus the bilinear coupling contribution γ^2/ac_{44}^0. The regular solution approximation leads to a prediction for the composition dependence of T_c, but it is not clear how to decompose Eq. (10) into separate components in order to generate the analog of Eq. (3). Thus we do not have a model prediction for $T_0(x)$. We will comment on this and other open questions in connection with the data analysis in Sec. IV.

III. EXPERIMENTAL PROCEDURE AND RESULTS

Single crystals of $K_xRb_{1-x}CN$ grown from the melt at the Crystal Growth Laboratory of the University of Utah were obtained from Professor F. Lüty. The samples studied were thin slabs ($1 \times 1 \times 0.25$ cm^3) cleaved from large single crystals. Terraces on the surfaces were polished down to give surface planarity and parallelity better than 1 μm, which is much smaller than the shortest wavelength $\lambda \simeq 30$ μm (corresponding to $v \simeq 300$ m/s, the smallest measured velocity).

Point defects surrounded by strains could be observed in the bulk of the crystal when a polished sample was investigated with a microscope using crossed polarizers. Between these pointlike strain sources there were homogeneous regions large enough to allow the application of an ultrasonic transducer with an effective active area of $\sim 3 \times 3$ mm^2.

Lithium niobate transducers were bonded to one crystal surface either with beeswax (230–300 K) or Dow

Corning 200 silicone fluid ($T < 230$ K). The transducers were always operated at their fundamental frequency of ~ 10 MHz. No experiments were attempted at higher frequencies. Because of differences in the thermal expansion of the transducer and the sample, samples frequently cracked at about 150–160 K upon slow cooling. This temperature is ~ 60 K below the freezing point of the silicone bond. These cleavage cracks developed perpendicular to the surface directly under the transducer. Due to the favorable orientation of such cracks, it was still possible in most cases to obtain reliable sound velocity data at lower temperatures.

Standard atomic-absorption spectra were used to determine the sample compositions, and the resulting x values were slightly different from the nominal compositions of the melts, as expected. Both sets of x values are given in Table I.

At the beginning of each run, the absolute sound velocity v at room temperature was determined with an estimated absolute accuracy of $\pm 1.5\%$, using the Papadakis pulse-overlap technique.[15] The room-temperature elastic constants $c_{44}(300 \text{ K}) = \rho v^2$ are shown in Table I. Relative changes in sound velocity as a function of temperature were detected with an accuracy of $\pm 10^{-3}\%$ using a computerized phase-sensitive MATEC MBS 800 system.[16] Cooling and warming runs were reproducible. No interesting behavior in the sound attenuation was observed during these runs. When a sample was cooled below the first-order phase transition, the acoustic signal decreased in magnitude abruptly, and then the signal reappeared at a slightly higher temperature upon warming. In two cases ($x = 0.37$ and 0.89) it was not possible to follow the acoustic signal all the way down to the first-order transition because the sample cracked at a higher temperature.

A liquid-nitrogen cryostat was used in the present experiments. The temperature of the sample was controlled by means of a manually set Bailey temperature controller. The temperature was stabilized for each data point over a period of 20–30 min and was measured with a calibrated platinum-resistance thermometer to within an accuracy of ± 2 mK.

A variety of data on the investigated mixed crystals is given in Table I together with data for the pure compounds. The room-temperature mass densities ρ were calculated using a linear interpolation between the KCN and RbCN values. The shear elastic constants c_{44} are shown as a function of temperature in Fig. 3. The elastic constant data for KCN ($x = 1$) and RbCN ($x = 0$) were

TABLE I. Various data for $K_xRb_{1-x}CN$ single crystals. The c_{44} values are given in units of 10^9 N/m^2 ($= 10^{10}$ dyn/cm^2) and the density ρ is in units of g cm^{-3}. The temperature T_{min} is the lowest temperature at which acoustic measurements could be made.

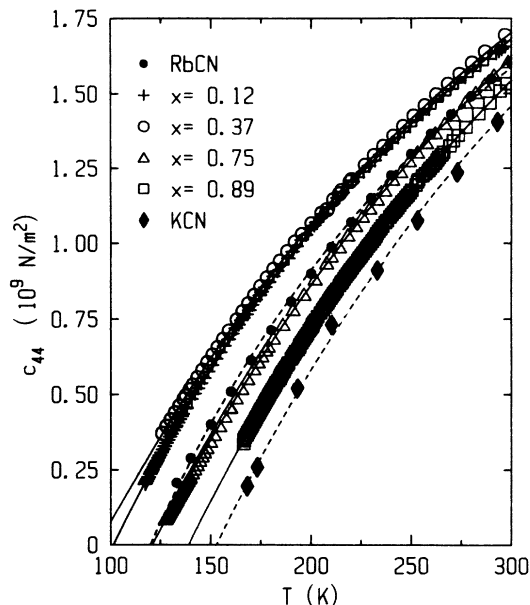| Analysis x	Nominal x_{nom}	ρ	$c_{44}(300 \text{ K})$	T_{min} (K)	$c_{44}(T_{min})$
0	0	2.314	1.652	133	0.213
0.12	0.1	2.238	1.655	117.0	0.1992
0.37	0.3	2.063	1.653	126.0	0.3594
0.75	0.75	1.768	1.534	127.5	0.0832
0.89	0.9	1.641	1.485	166.6	0.3509
1	1	1.558	1.405	168	0.195

FIG. 3. Shear elastic constant c_{44} as a function of temperature for KCN, RbCN, and $K_x Rb_{1-x} CN$ mixed crystals. The dashed lines represent CW fits to the two pure compounds; the solid lines are RF2 fits to the mixed crystal data. See text for a description of the fitting procedure.
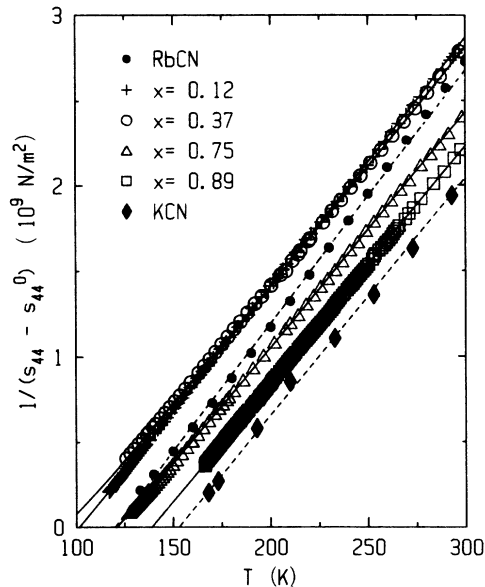

FIG. 4. Temperature dependence of the inverse excess shear compliance $(s_{44} - s_{44}^0)^{-1}$, where $s_{44}^0 \equiv 1/c_{44}^0$ is the bare compliance in the absence of translation-rotation coupling. The values of c_{44}^0 used to obtain these plots are those listed in Table II. The dashed lines represent CW fits to the pure compounds and the solid lines are RF1 fits to the mixed-crystal data.

taken from Refs. 9 and 10.[17] The solid and dashed lines represent theoretical fits to the data as described in Sec. IV.

IV. DATA ANALYSIS AND DISCUSSION

It is clear from an inspection of Figs. 3 and 4 that the elastic behavior of the mixed-crystal samples is substantially different from a simple interpolation between the two pure compounds. In particular, the transition temperatures are lower than expected from Eq. (7a) and the temperature dependencies $c_{44}(T)$ are also different. The latter aspect is most obvious for the samples with $x=0.37$ and 0.75, which is not surprising since deviations from ideal behavior are proportional to the quantity $x(1-x)$.

There are two possible sources of the nonideal elastic behavior for $K_x Rb_{1-x} CN$ crystals: (1) quenched random strain fields that give rise to a nonzero Edwards-Anderson order parameter $q(T)$ given by Eq. (5), and (2) $CN^- - CN^-$ pair interaction energies that depend on cationic occupancy and thus give rise to a nonzero value of the ΔT_c^{KRb} parameter appearing in Eqs. (10) and (11). We first tested the possibility that the observed behavior of $K_x Rb_{1-x} CN$ crystals was completely due to random field effects $(q \equiv \Sigma / T^2 \neq 0, \Delta T_c^{KRb} = 0)$. Such attempts to fit the data with Eqs. (5)–(7) were unsuccessful. No detailed specification of parameters will be given since the X_ν^2 values were very high and large systematic deviations occurred.[18] Next, we tested the possibility that nonideal $K_x Rb_{1-x} CN$ behavior was completely due to the weakening of the effective $CN^- - CN^-$ coupling when different-sized cations occupied the sites adjacent to a given CN^- pair $(q=0, \Delta T_c^{KRb} \neq 0)$. Such fits will be

denoted Curie-Weiss (CW) fits. We used the simple CW elastic expression given in Eq. (2) with c_{44}^0, T_c, and T_0 as freely adjustable parameters, and then checked whether the resulting $T_c(x)$ values obey Eq. (10). The least-squares parameters obtained from the CW fits are given in Table II and displayed graphically in Figs. 5–8. A discussion of the composition dependence of these parameters and their physical plausibility is presented below, but it should be noted now that we do not consider the CW fits as a very satisfactory representation of the nonideal behavior. In particular, note the large bare stiffnesses c_{44}^0 for the $x=0.37$ and 0.75 samples; such artificially large values are required to obtain a linear $(s_{44} - s_{44}^0)^{-1}$ temperature dependence at these concentrations.

Another representation of the elastic behavior in $K_x Rb_{1-x} CN$ is based on allowing both random strain fields and nonideal T_c effects to play a role $(q \neq 0$ and $\Delta T_c^{KRb} \neq 0)$. Such fits, denoted random-field (RF) fits, are based on Eq. (6) with $q = \Sigma / T^2$, the adjustable parameters being c_{44}^0, T_c, T_0, and Σ. We have carried out two variants: RF1, for which $T_0(x)$ is taken to follow a linear interpolation between the two pure cyanides as given by Eq. (7b), and RF2, for which $T_c(x) - T_0(x)$ is taken to follow a linear interpolation. Because of coupling among the parameters when both random strain fields and regular solution effects are allowed, it is necessary to introduce such constraints to ensure convergence to a well-defined X^2 minimum for which $\Sigma > 0$. The choice of these constraints is somewhat arbitrary. One could also take the c_{44}^0 values or the quantity γ^2 / α to be linear interpolations between the values for KCN and RbCnN, but these choices yield fits that are essentially the same as RF2 in

TABLE II. Values of the adjustable parameters c_{44}^0 (the bare elastic constant in units of 10^9 N/m²), T_c, T_0, and Σ appearing in Eqs. (5) and (6) for Curie-Weiss (CW) and random-field (RF) fits to K_xRb_{1-x}CN data. Values of $T_c - T_0$ and $q_{max} = \Sigma/T_{min}^2$ are also given.

χ	Fit	c_{44}^0	T_c (K)	T_0 (K)	$T_c - T_0$ (K)	Σ (K²)	q_{max}	χ_ν^2
0	CW	3.887	119.9	−141.2	261.1	0		
0.12	CW	3.965	102.7	−168.1	270.8	0		1.36
	RF1	3.936	109.8	(−150.0)	259.8	767	0.056	1.63
	RF2	4.051	108.1	−165.7	(273.8)	627	0.046	2.20
0.37	CW	4.643	95.6	−256.6	352.2	0		1.05
	RF1	4.167	112.0	(−168.3)	280.3	1536	0.107	1.54
	RF2	4.303	107.4	−193.0	(300.3)	1131	0.087	1.32
0.75	CW	5.253	121.2	−279.7	401.0	0		2.00
	RF1	4.733	133.7	(−196.0)	329.8	1411	0.084	1.00
	RF2	4.819	132.1	−208.6	(340.6)	1240	0.069	1.14
0.89	CW	4.958	139.5	−216.3	355.8	0		1.02
	RF1	4.964	144.2	(−206.3)	350.5	711	0.026	1.19
	RF2	5.002	143.2	−212.2	(355.5)	581	0.021	1.19
1	CW	5.100	152.8	−214.3	367.1	0		

terms of χ_ν^2 and parameter values. The least-squares-fitting parameters from the RF1 and RF2 fits are listed in Table II and displayed in Figs. 5–8. Quantities held fixed at the specified values are enclosed in parentheses.

These RF fits are not better in a statistical sense than the CW fits, but they show that satisfactory fits to the data are possible using parameters that exhibit a physically attractive pattern of composition dependence. The present data are compatible with any of the three fits. Figures 3 and 4 show the character of the agreement between observed and calculated values obtained with RF1 and RF2 fits, and CW fits yield equivalent or slightly

better agreement. In all three fits, a substantial nonlinear variation in $T_c(x)$ is required, which establishes that $J_{KRb} \neq \frac{1}{2}(J_{KK} + J_{RbRb})$ and ΔT_c^{KRb} must be nonzero. The values of the parameter $T_c(x)$ were fitted with Eq. (10). The resulting parabolic curves are shown in Fig. 6, and the ΔT_c^{KRb} values are given in Table III along with T_c^{KRb} values obtained from Eq. (11) using $\frac{1}{2}(T_c^{KK} + T_c^{RbRb})$ $= \frac{1}{2}(142.8 + 119.9) = 136.4$ K. The values of Σ_0 obtained from fitting Σ with $\Sigma = x(1-x)\Sigma_0$ are also listed in Table III.

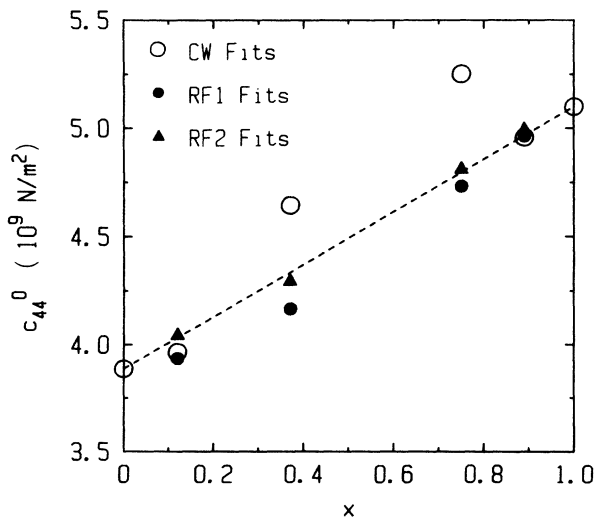In our view, the fits RF1 and RF2, which include a

FIG. 5. Composition dependence of the bare elastic constant c_{44}^0 obtained from various fits to the experimental data.
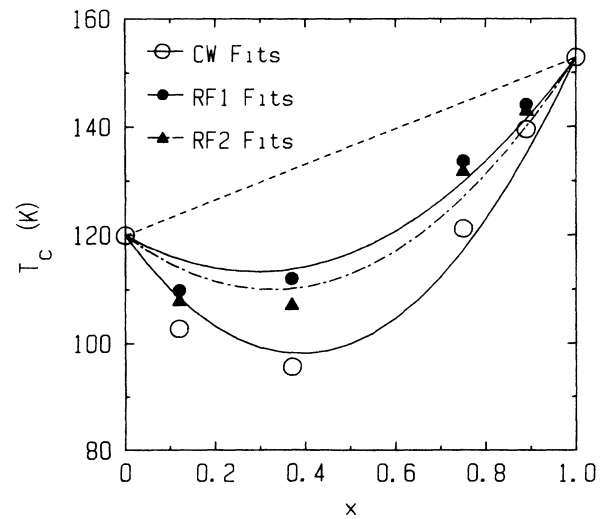

FIG. 6. Composition dependence of the critical temperature T_c for quadrupolar ordering. The three parabolic curves represent fits to these $T_c(x)$ values with Eq. (10).
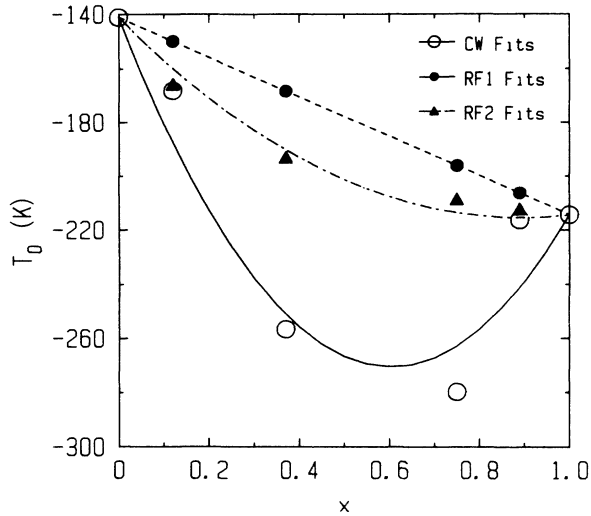
C. W. GARLAND, J. O. FOSSUM, AND A. WELLS

FIG. 7. Composition dependence of the parameter T_0. For RF1 fits, the T_0 values were held fixed at the linear interpolation values indicated on the dashed line. The two parabolic curves represent fits to the CW and RF2 parameters with $T_0(x) = xT_c^{KK} + (1-x)T_c^{RbRb} - 2x(1-x)\Delta T_0^{KRb}$, the analog of the regular solution form for $T_c(x)$ given in Eq. (10).

TABLE III. Values of the parameters ΔT_c^{KRb}, T_c^{KRb}, and ΔT_0^{KRb}, all in K, and Σ_0 in units of K^2.

Type of fit	ΔT_c^{KRb}	T_c^{KRb}	ΔT_0^{KRb}	Σ_0
CW	72.9	63.5	177.8	0
RF1	39.4	97.0	0	7260
RF2	47.0	89.4	47.0	5935

$\gamma^2/\alpha = c_{44}^0(T_c - T_0)$, as shown in Figs. 5 and 9. Finally, the RF fits require a less drastic nonideality in the $T_c(x)$ and $T_0(x)$ values; see Figs. 6 and 7 and Table III.

random-strain-field contribution, are more physically plausible than the CW fits. Elastic measurements on the diluted cyanides $RbCN_xBr_{1-x}$, KCN_xBr_{1-x}, and KCN_xCl_{1-x} have demonstrated the existence of an Edwards-Anderson order parameter with Σ_0 values of 2317, 2500, and 11 000 K^2, respectively.[8] Thus, the magnitude of the Σ_0 value found here, 6000–7000 K^2, seems reasonable. Furthermore, the RF fits yield an almost linear variation for the model parameters c_{44}^0 and

V. SUMMARY

The c_{44} shear elasticity of $K_xRb_{1-x}CN$ mixed crystals in the high-temperature (disordered) cubic phase has been measured and analyzed as a function of temperature and composition. The critical temperature $T_c(x)$ for long-range quadrupolar ordering exhibits a pronounced and roughly parabolic dependence on x. This T_c variation, which indicates that the effective CN^--CN^- lattice-mediated quadrupolar coupling constant is sensitive to the nature of the cations occupying adjacent sites, can be modeled empirically by a "regular solution" expression [Eq. (10)]. The temperature dependence of c_{44} for any given sample can be fitted with either a simple elastic Curie-Weiss law [Eq. (2)] or an extended mean-field model that includes quenched random strain fields [Eq. (6)]. The composition dependencies of the resulting fit parameters are more attractive for the RF fits, but the CW fits cannot be excluded on the basis of the present data.
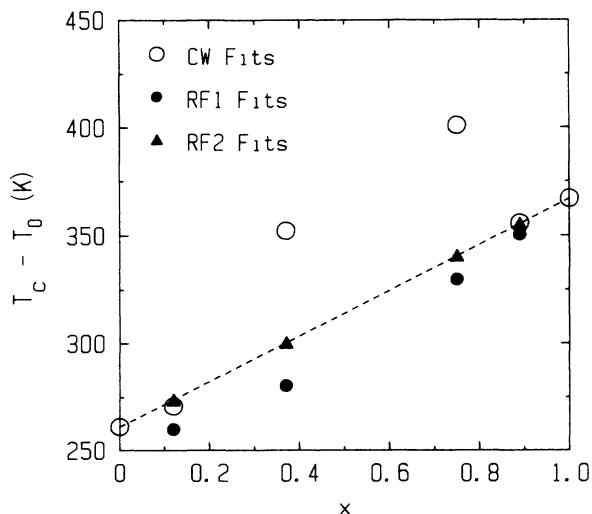

FIG. 8. Composition dependence of $T_c - T_0 = \gamma^2/\alpha c_{44}^0$. For RF2 fits, the $T_c - T_0$ values were held fixed at the linear interpolation values indicated on the dashed line.
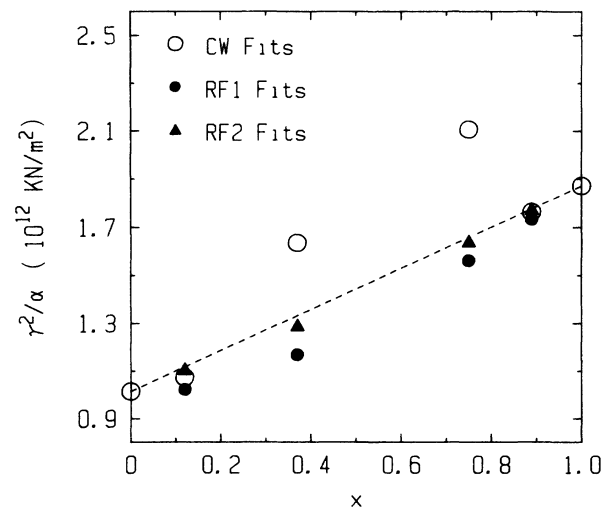

FIG. 9. Composition dependence of the quantity γ^2/α, where α and γ are coefficients in the Landau free energy given in Eq. (1).

[1]F. Lüty, in *Defects in Insulating Crystals,* edited by V. M. Turkevich and K. K. Svarts (Springer-Verlag, Berlin, 1981), pp. 69–89.

[2]F. Lüty and J. Ortiz-Lopez, Phys. Rev. Lett. **50**, 1289 (1982).

[3]K. H. Michel and J. M. Rowe, Phys. Rev. B **32**, 5818 (1985); **32**, 5827 (1985).

[4]The low-temperature ordered structure is monoclinic for RbCN and orthorhombic for KCN. The orientationally ordered structures in $K_x Rb_{1-x}CN$ depend on composition and temperature in a complex way. J. Ortiz-Lopez and F. Lüty, Phys. Rev. B **37**, 5461 (1988).

[5]U. G. Volkmann, R. Bohmer, A. Loidl, K. Knorr, U. T. Hochli, and S. Haussühl, Phys. Rev. Lett. **56**, 1716 (1986).

[6]K. H. Michel, Phys. Rev. Lett. **57**, 2188 (1986).

[7]K. H. Michel, Phys. Rev. B **35**, 1405 (1987); **35**, 1414 (1987); Z. Phys. B **68**, 259 (1987).

[8]J. O. Fossum and C. W. Garland, Phys. Rev. Lett. **60**, 592 (1988).

[9]S. Haussühl, Solid State Commun. **13**, 147 (1973); S. Haussühl, J. Eckstein, K. Recker, and F. Wallrafen, Acta Crsytallogr. Sect. A **33**, 847 (1977).

[10]S. Haussühl, Solid State Commun. **32**, 181 (1979).

[11]J. Z. Kwiecien, R. C. Leung, and C. W. Garland, Phys. Rev. B **23**, 4419 (1981).

[12]R. Feile, A. Loidl, and K. Knorr, Phys. Rev. B **26**, 6875 (1982).

[13]R. Folk, H. Iro, and F. Schwabl, Z. Phys. B **25**, 69 (1976).

[14]J. O. Fossum, A. Wells, and C. W. Garland, Phys. Rev. B **38**, 412 (1988).

[15]E. P. Papadakis, J. Acoust. Soc. Am. **42**, 1045 (1967).

[16]P. W. Wallace and C. W. Garland, Rev. Sci. Instrum. **57**, 3085 (1986).

[17]As disucssed in Ref. 14, the c_{44} data for RbCN given in Ref. 10 appear to be systematically high by about 3%. Thus we have used "corrected" $c_{44}(T)$ values obtained by multiplying each reported value by the constant factor 0.97.

[18]For these fits, an extremely large ($\sim 20\,000$) Σ_0 value was needed to produce the required low values of $T_c(1-q)$, but this led to an inappropriate temperature dependence of c_{44}. Even if the constraint (7b) on $T_0(x)$ was relaxed and $T_0(x)$ was allowed to be freely adjustable, no satisfactory fits could be achieved with Eqs. (5), (6), and (7a).